NASA-CR-199978

WASHINGTON UNIVERSITY

DEPARTMENT OF PHYSICS

LABORATORY FOR ULTRASONICS

St. Louis, Missouri 63130

"Application of Linear Array Imaging Techniques to the Real-Time Inspection of Airframe Structures and Substructures"

Annual Progress Report: March 15, 1995 - October 31, 1995

NASA Grant Number: NSG-1601

Principal Investigator:

Dr. James G. Miller

Professor of Physics

The NASA Technical Officer for this grant is:

Dr. Patrick H. Johnston

NASA Langley Research Center

Hampton, Virginia

(NASA-CR-199978) APPLICATION OF LINEAR ARRAY IMAGING TECHNIQUES TO THE REAL-TIME INSPECTION OF AIRFRAME STRUCTURES AND SUBSTRUCTURES Annual Report, 15 Mar. - 31 Oct. 1995 (Washington Univ.) 19 p

N96-19514

Unclas

G3/38 0101204

Application of Linear Array Imaging Techniques to the Real-Time Inspection of Airframe Structures and Substructures

I. Introduction

In this Progress Report, we describe our further development and application of linear array imaging technologies to address specific aging-aircraft inspection issues. We present real-time video-taped images obtained from an unmodified commercial linear-array medical scanner of specimens constructed to simulate typical types of flaws encountered in the inspection of aircraft structures.

In Section II of this Progress Report we describe the method of linear-array imaging. This section briefly reviews how the images were obtained. Section III describes the specific specimens investigated followed by a discussion of the observations in Section IV. Results of the linear array imaging are presented on an accompanying videotape.

II. Method of Linear-Array Imaging

An unmodified, commercially available Hewlett-Packard Sonos 2500 medical linear array imaging system was employed. The Sonos 2500 was operated in a mode that utilized a linear array of ultrasonic transducer elements as the interrogating probe. The B-scan (cross-sectional) image of the object under interrogation was formed by sequentially transmitting and receiving with groups of transducer elements across the array. Each transmission of an ultrasonic pulse and the subsequent reception of the returned signals by a specific group of transducers represents one ultrasonic A-line in a direction normal to the array. The B-scan image is produced from a series of A-lines across the aperture of the array. A depth-dependent gain (time-gain compensation or TGC) was applied to the received ultrasonic signals to reduce the effects due to the inherent attenuation of the specimen on the displayed B-scan image.

The ultrasonic signals obtained with the linear array are logarithmically compressed and displayed as a gray scale image on a dB scale. In general, each B-scan image obtained with a linear array is a cross-sectional representation of the amplitude of the reflected (scattered) ultrasonic signals, in the plane of the array, throughout the depth of the specimen under interrogation.

Because the Sonos 2500 system is intended to be used to image specific organs, vessels, and tissues in a clinical setting, it was not possible to change the depth setting of the images to more closely correspond to the thickness dimensions of the specimens. Therefore, the images obtained with the Sonos 2500 system typically represent the echo-decay patterns of many round-trip echoes. Interpretation of the images obtained from relatively thin or layered solids were expected to be somewhat complex because of the presence of strong reverberations and possible mode conversions. Because the linear array imaging system currently available is a 7.5 MHz imagining system, the test specimens were scaled such that the dimensions were more appropriate for 7.5 MHz interrogation. This does not compromise the results of the investigation or the applicability of the linear array imaging technique to actual aircraft structures but permits us to investigate the usefulness of linear array imaging on proportionately sized specimens.

III. Specimens Investigated

A Hewlett-Packard Sonos 2500, configured in the 7.5 MHz linear array imaging mode, was employed to interrogate a series of specimens with intentional flaws. One genre of specimen contained simulated "cracks" under fasteners. Flat-bottom holes were drilled under the fasteners (3/8" 10-32 machine screws) to represent cracks in a plane parallel to the face of the linear array probe. These specimens were interrogated in a water bath with the linear array insonifying the top surface of the specimen as illustrated in Figure 1. Duplicate flat-bottom holes were drilled midway between the fasteners to aid in the initial determination of the type of echo the investigator should look for. The dimensions of the fasteners and the simulated cracks for this type of specimen are also displayed in the figure.

Specimens designed to mimic a typical "I"-shaped stiffener support structure component (that might be found as part of the underlying airframe substructure) were investigated next. In airframe applications the flange of a stiffener is typically attached to the skin of the structure it is supporting, thus ultrasonic inspections are limited to accessing the "I"-beam through one of its flanges. To simulate the cracks in this type of support structure, flat-bottom holes were drilled in the flange and web regions as well as the region where the web connects to the flange, (referred to as the radius region). Due to the availability of material aluminum "T" 's were substituted for the "I"-shaped stiffeners. Figure 2 displays the aluminum sample dimensions and Figures 3,4,5 depict the measurement setups. Specific details describing the flaw sizes, locations and imaging observations are summarized in Tables 2,3,4.

Linear array imaging techniques were applied to the interrogation of solid aluminum angles ("L" stiffeners) with flat-bottom holes of specific diameters drilled into the radius of the inclusive and exclusive angle of the "L" as depicted in Figures 6 and 7. The radii were interrogated with the right-angle specimens immersed in a water bath and the linear array positioned from the opposite side to which the flat-bottom hole was drilled. The linear array was oriented such that the images produced were formed with the array orthogonal to the plane of the right-angle. Table 5 summarizes the flaw sizes interrogated.

IV. Discussion of Observations

In this Section we summarize the findings from our interrogation of the specimens described above. The accompanying video tape displays the linear array observations in detail.

Table 1 summarizes the observations for the linear array interrogations of the specimen containing flaws under the head of fasteners. The echoes from the flat-bottom holes under a fastener appear as short horizontal lines located between the initial front wall reflection and the first back wall reflection. All of the flaws (1/8", 1/16", and 1/32" flat-bottom holes) were discernible but the echoes decreased in brightness the smaller the hole diameter.

The observations for the linear array interrogations of flaws in the flange of "T"-shaped stiffener support structures are summarized in Table 2. The linear array was mounted to a gelatin standoff and positioned across the web of the stiffener as shown in Figure 3. The B-scan image displayed parallel horizontal lines on the left and right side of the image and a darkened region in the center of the image. The horizontal lines (echoes) represent the reverberations from the back wall of the flanges and the darkened center region the web area of the specimen. All the flat-bottom hole echoes appear as a reverberation pattern of short horizontal lines. The first echo of the pattern appears approximately midway between the front wall echo and first back wall echo from the flanges. The flaws for all the diameter flat-bottom holes were observed.

Table 3 summarizes the observations for the linear array interrogations of flaws in the web of "T"-shaped stiffener support structures. The linear array was mounted to a gelatin standoff and positioned across the web of the stiffener as illustrated in Figure 4. The B-scan image displayed parallel horizontal lines on the left and right side of the image and a darkened region in the center of the image. Again the horizontal lines (echoes) represent the reverberations from the back wall of the flanges and the darkened center region the web area of the specimen. All the flat-bottom hole echoes appear as a reverberation pattern of short horizontal lines in the darkened center region (the web region). Detection of all the flaws was achieved except for the deepest 1/4", 1/8", and the 1/32" flaws.

The observations for the flaws in the radius of "T"-shaped stiffener support structures are summarized in Table 4. The linear array was mounted to a gelatin standoff and positioned aligned along the web of the stiffener and tilted approximately 5° with respect to the normal of the flange, as depicted in Figure 5. The echo decay pattern from the flaw appears as a series of short horizontal lines interspersed with the series of horizontal lines (echoes from where the flange connects with the web). Echoes from the flaws were most easily seen when the ultrasound impinged on the flaw perpendicular to an aluminum/flaw interface. Therefore, the slight tilting of the linear array helped to brighten the flaws echo. Detection of all the flaws was achieved except for the 1/8", 65° flaw.

Table 5 summarizes the observations for the linear array interrogations of flaws in the radius of "L"-shaped stiffener support structures. The specimens were interrogated in a water bath as illustrated in Figures 6 and 7.

The typical B-scan image for flaws drilled into the inclusive angle of the radius and insonified from the exclusive angle side displayed a wide band of white (corresponding to the initial water/specimen interface) followed by horizontal lines. The flaw appeared as a short horizontal line lying between the wide band and the horizontal line. Detection of the 1/4", 1/8", and the 1/16" flaws was achieved, but not for the 1/32" flaw.

The typical B-scan image for flaws drilled into the exclusive angle of the radius and insonified from the inclusive angle side displayed a series of parallel horizontal lines with the flaw represented by two echo decay patterns side be side. Each echo decay pattern consisted of short horizontal lines. The two echo decay patterns were horizontally separated by a short dark space.
Detection was achieved for the 1/4", 1/8", and the 1/16" flaws, but not for the 1/32" flaw.

V. Conclusion

These results suggest that information regarding the characteristics, location, and interface properties of specific types of flaws in materials and structures may be obtained from the images acquired with a linear array. Furthermore, linear array imaging may offer the advantage of being able to compare "good" regions with "flawed" regions simultaneously, and in real time. Real-time imaging permits the inspector to obtain image information from various views and provides the opportunity for observing the effects of introducing specific interventions. Observation of an image in real-time can offer the operator the ability to "interact" with the inspection process, thus providing new capabilities, and perhaps, new approaches to nondestructive inspections. This enhancement may aid in the probability of detection and real-time characterization of certain types of flaws.

Flat-Bottom Hole Under Head of Fastener

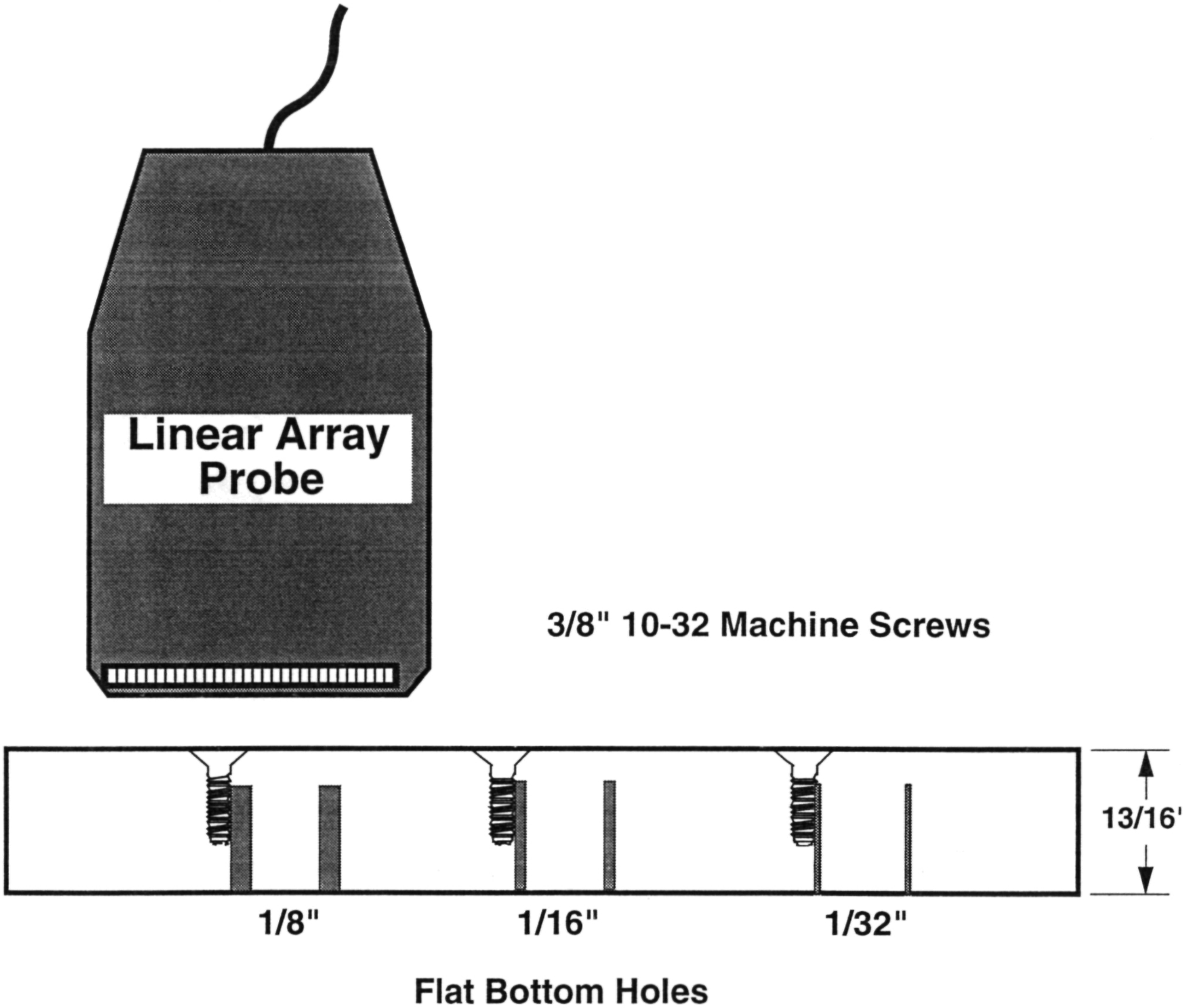

Figure 1: Illustration of the measurement setup for the interrogation of "flaws" located under the head of fasteners

Aluminum "T" Dimensions

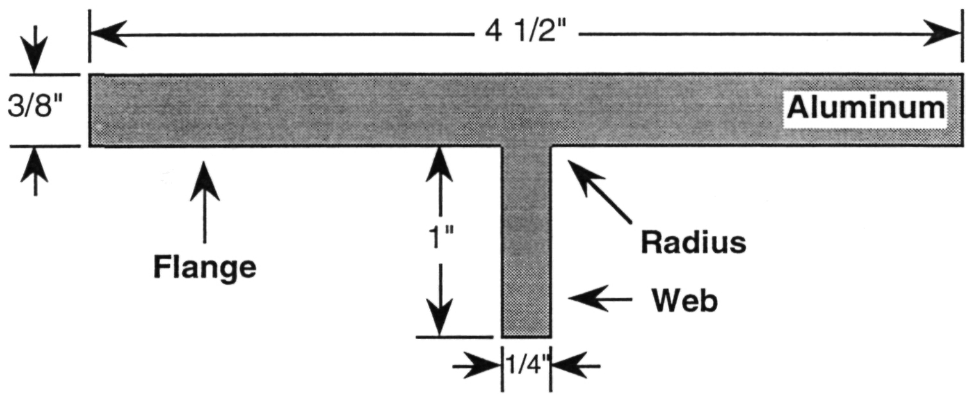

Figure 2: Sample dimensions for the interrogation of "flaws" in the flange, web, and radius of "I"-shaped stiffener support structures. "T"-shaped aluminum samples were substituted for the "I"-shaped stiffener.

Flat-Bottom Hole in Flange

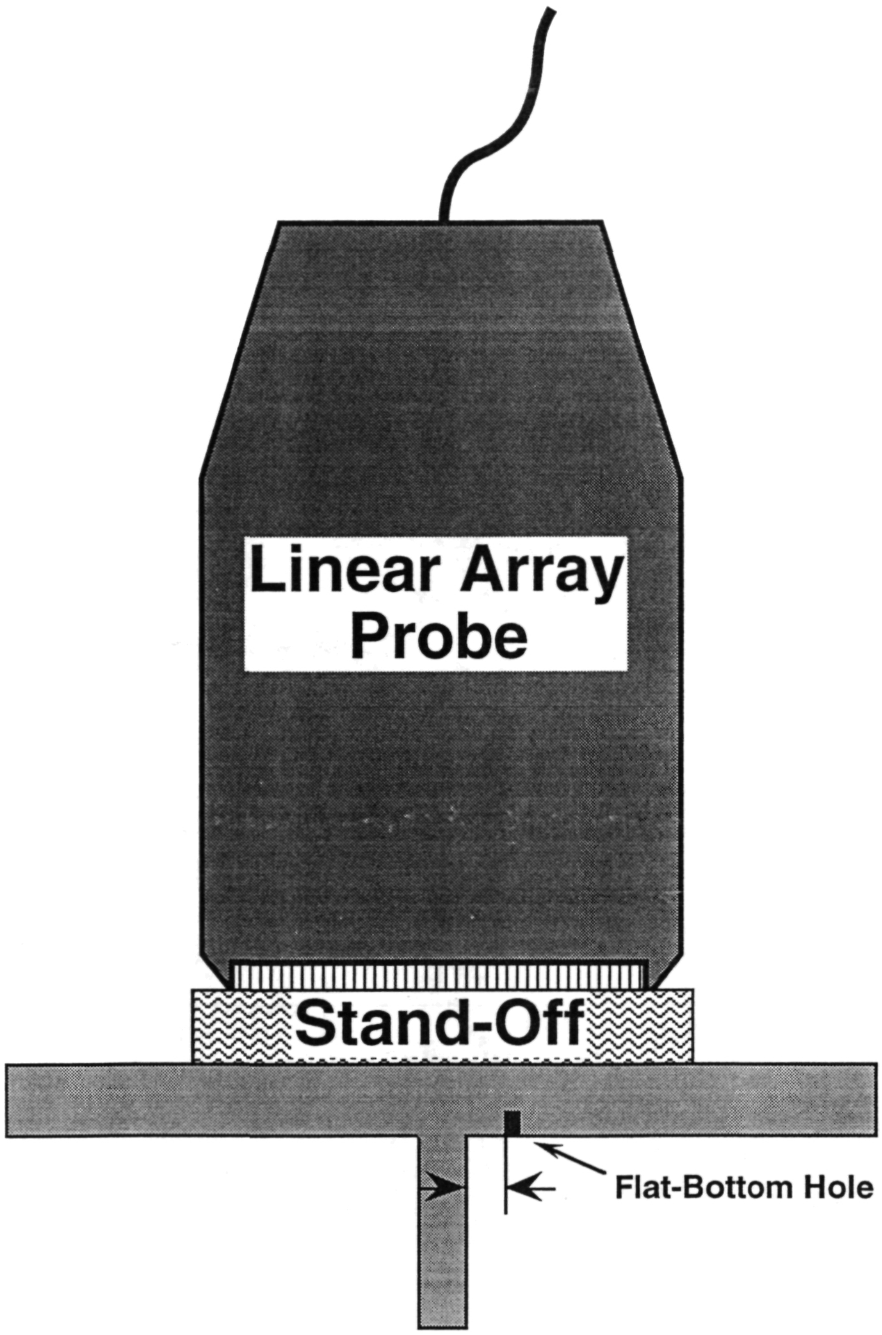

Figure 3: Illustration of the measurement setup for the interrogation of "flaws" in the flange of a stiffener support structure

Flat-Bottom Hole in Web

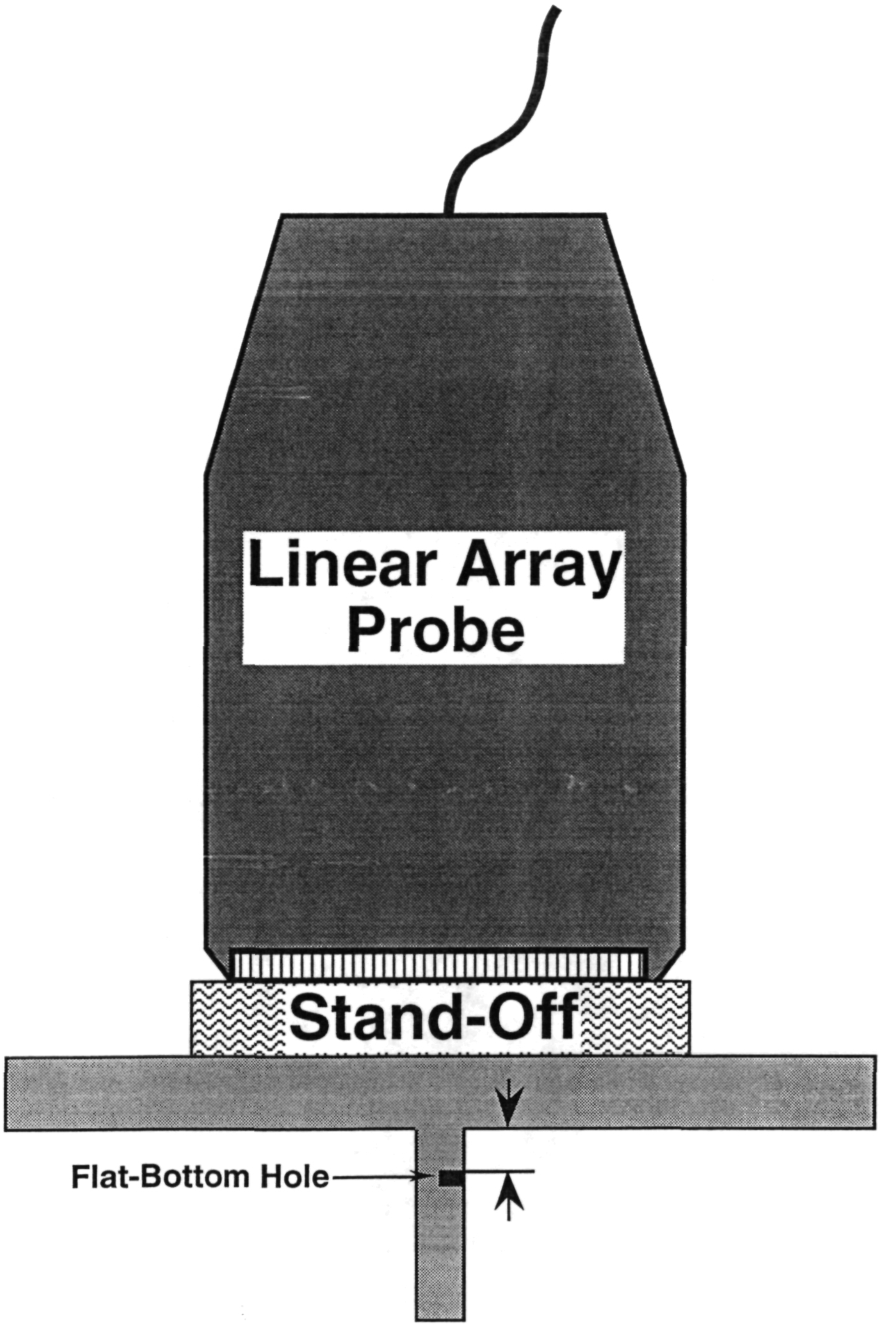

Figure 4: Illustration of the measurement setup for the interrogation of "flaws" in the web of a stiffener support structure

Flat-Bottom Hole in Radius

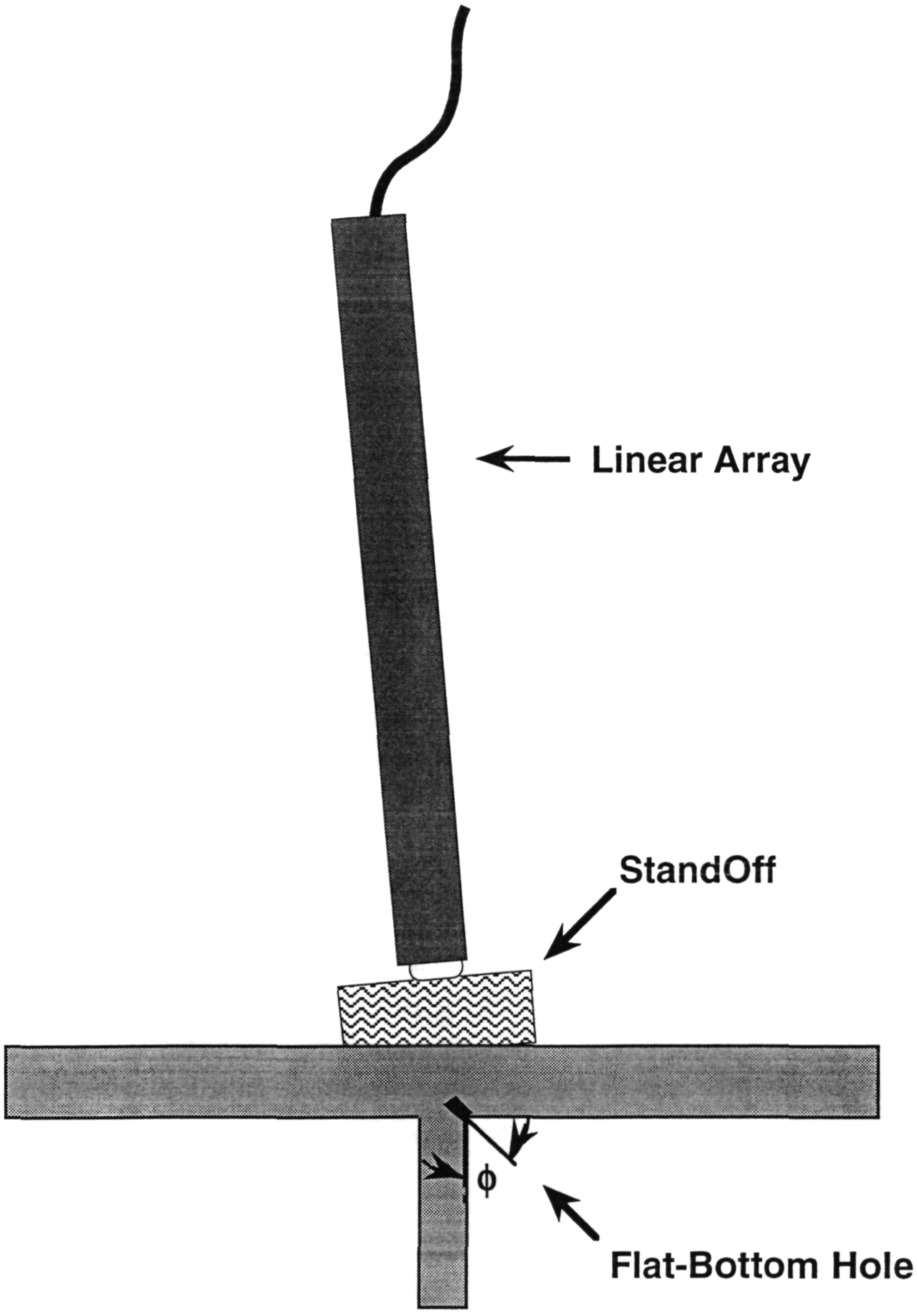

Figure 5: Illustration of the measurement setup for the interrogation of "flaws" in the radius of a stiffener support structure

Flat-Bottom Hole in Inclusive Angle of "L"-Shape Stiffener

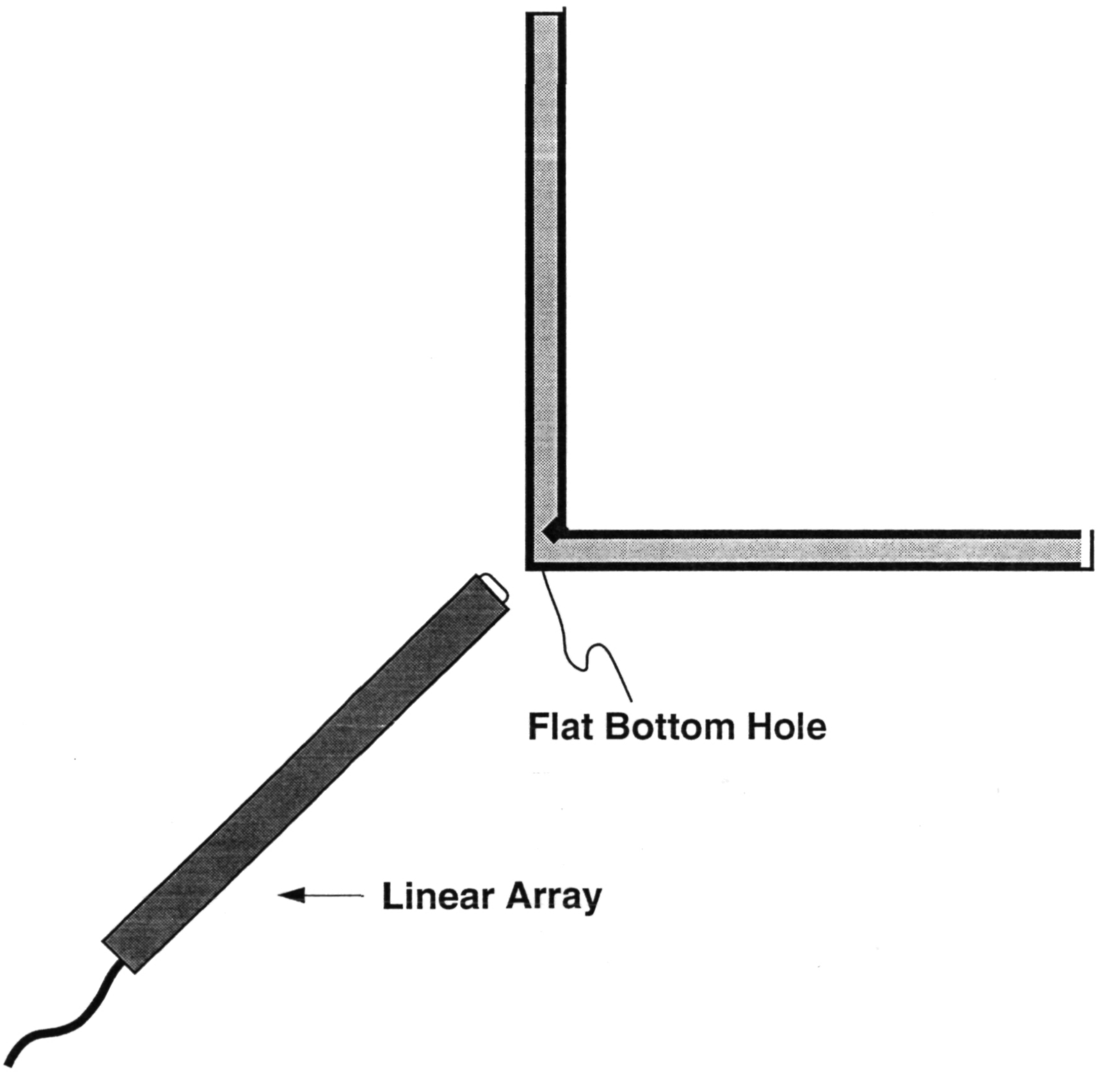

Figure 6: Illustration of the measurement setup for the interrogation of "flaws" in the inclusive angle of an "L"-shaped stiffener

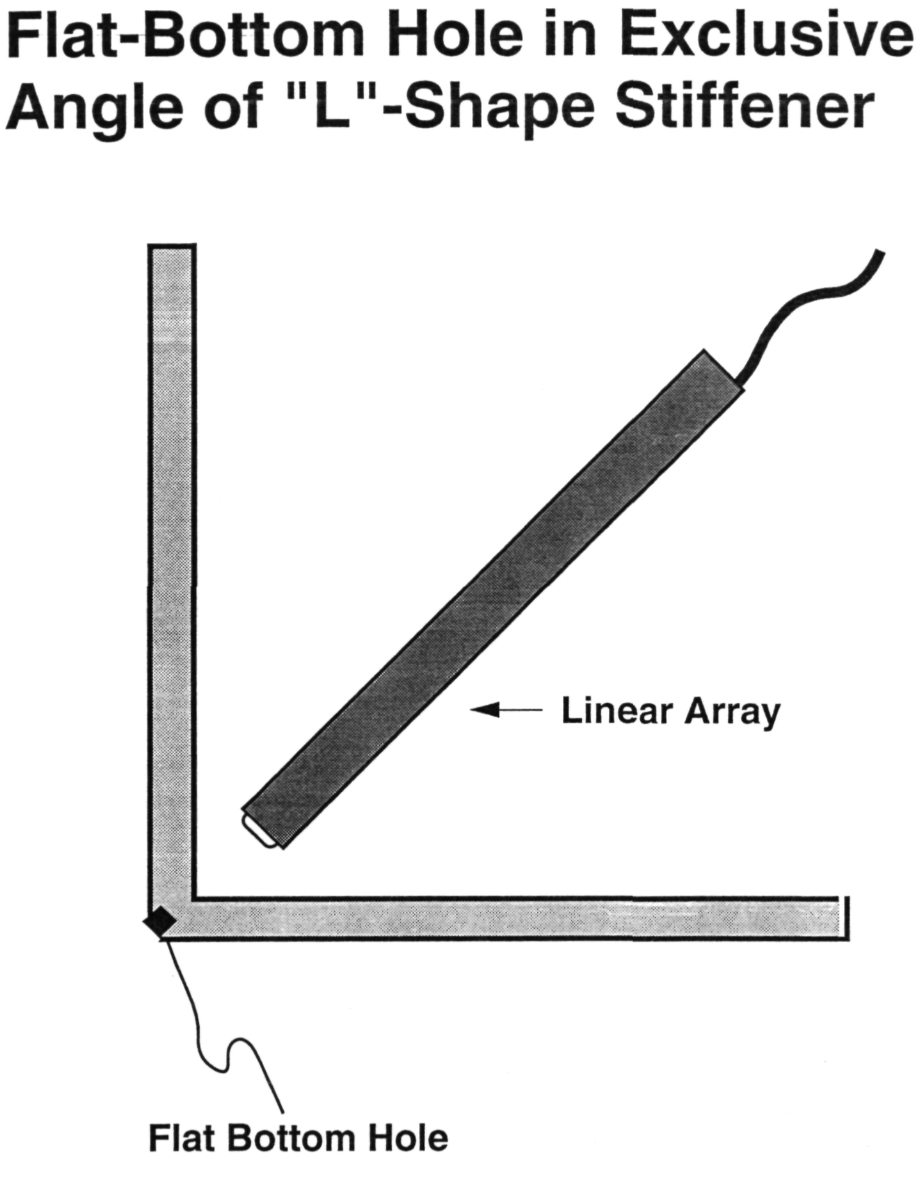

Figure 7: Illustration of the measurement setup for the interrogation of "flaws" in the exclusive angle of an "L"-shaped stiffener

Flat-Bottom Hole Under Head of Fasteners (3/8" 10-32 machine screws were used for the fasteners)	
Flat-Bottom Hole Diameter	**Was the Flaw Seen?**
1/8"	yes
1/16"	yes
1/32"	no

Table 1: Summary of the observations for the interrogation of "flaws" under the head of a fastener with the linear array imaging system

Flat-Bottom Hole in Flange of "T"		
Flat-Bottom Hole Diameter	**Flat-Bottom Hole Location in the Flange (distance from outer diameter of flat-bottom hole to the side surface of the web)**	**Was the Flaw Seen?**
1/4"	0 mm	yes
1/4"	6 mm	yes
1/4"	12 mm	yes
1/4"	15 mm	yes
1/4"	18 mm	yes
1/8"	0 mm	yes
1/8"	4 mm	yes
1/8"	10 mm	yes
1/8"	13 mm	yes
1/8"	16 mm	yes
1/16"	0 mm	yes
1/16"	4 mm	yes
1/16"	7 mm	yes
1/16"	10 mm	yes
1/16"	13 mm	yes
1/32"	0 mm	yes
1/32"	3 mm	yes
1/32"	6 mm	yes
1/32"	9 mm	yes
1/32"	12 mm	yes

Table 2: Summary of the observations for the interrogation of "flaws" in the flange of a "T"-shaped stiffener with the linear array imaging system

Flat-Bottom Hole in Web of "T"		
Flat-Bottom Hole Diameter	**Flat-Bottom Hole Location in the Web (distance from outer diameter of flat-bottom hole to the bottom surface of the flange)**	**Was the Flaw Seen?**
1/4"	0 mm	yes
1/4"	6 mm	yes
1/4"	13 mm	yes
1/4"	18 mm	no
1/8"	0 mm	yes
1/8"	7 mm	yes
1/8"	13 mm	yes
1/8"	20 mm	no
1/16"	0 mm	yes
1/16"	7 mm	yes
1/16"	14 mm	yes
1/16"	20 mm	yes
1/32"	0 mm	yes
1/32"	6 mm	yes
1/32"	12 mm	yes
1/32"	18.5 mm	no

Table 3: Summary of the observations for the interrogation of "flaws" in the web of a "T"-shaped stiffener with the linear array imaging system

Flat-Bottom Hole in Radius of "T"		
Flat-Bottom Hole Diameter	**Flat-Bottom Hole Angle in the Web (angle measured with respect to the web)**	**Was the Flaw Seen?**
1/4"	0 degrees	yes
1/4"	25 degrees	yes
1/4"	45 degrees	yes
1/4"	65 degrees	yes
1/4"	90 degrees	yes
1/8"	0 degrees	yes
1/8"	25 degrees	yes
1/8"	45 degrees	yes
1/8"	65 degrees	no
1/8"	90 degrees	yes
1/16"	0 degrees	yes
1/16"	25 degrees	yes
1/16"	45 degrees	yes
1/16"	65 degrees	yes
1/16"	90 degrees	yes
1/32"	0 degrees	yes
1/32"	25 degrees	yes
1/32"	45 degrees	yes
1/32"	65 degrees	yes
1/32"	90 degrees	yes

Table 4: Summary of the observations for the interrogation of "flaws" in the radius of a "T"-shaped stiffener with the linear array imaging system

Flat-Bottom Hole in the Radius of an "L"-Stiffener		
Flat-Bottom Hole Diameter	**Flat-Bottom Hole Location**	**Was the Flaw Seen?**
1/4"	Drilled in the inclusive angle	yes
1/8"	Drilled in the inclusive angle	yes
1/16"	Drilled in the inclusive angle	yes
1/32"	Drilled in the inclusive angle	no
1/4"	Drilled in the exclusive angle	yes
1/8"	Drilled in the exclusive angle	yes
1/16"	Drilled in the exclusive angle	yes
1/32"	Drilled in the exclusive angle	no

Table 5: Summary of the observations for the interrogation of "flaws" in the radius of a "L"-shaped stiffener with the linear array imaging system